Linnaeus University Dissertations
No 634/2026

Anuthariq Alikkam Veetil

Engineering Protein Binders for the Transferrin Receptor

From Viral Decoys to Delivery Vehicles

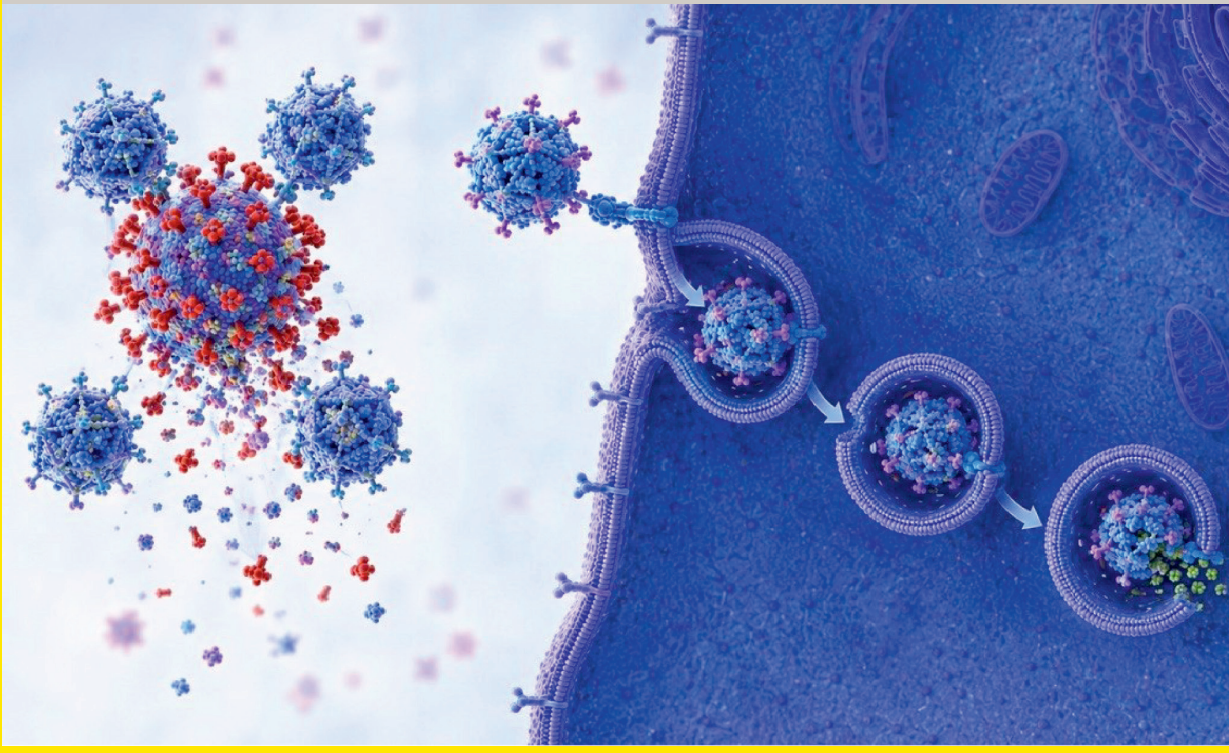

LINNAEUS UNIVERSITY PRESS

Engineering Protein Binders for the Transferrin Receptor

From Viral Decoys to Delivery Vehicles

Linnaeus University Dissertations

No 634/2026

Engineering Protein Binders for the Transferrin Receptor

From Viral Decoys to Delivery Vehicles

Anuthariq Alikkam Veetil

LINNAEUS UNIVERSITY PRESS

The doctoral dissertation seminar will be held at 09:15, on 13 November 2026 in room Azur, House Vita, Kalmar. The opponent will be Dr. Fabio Parmeggiani Cardiff University, UK.

Engineering Protein Binders for the Transferrin Receptor: From Viral Decoys to Delivery Vehicles

Doctoral dissertation, Department of Chemistry and Biomedical Sciences, Linnaeus University, Kalmar, 2026

ISBN: 978-91-8082-506-1 (print), 978-91-8082-507-8 (pdf)
© Anuthariq Alikkam Veetil
DOI: https://doi.org/10.15626/LUD.634.2026
Published by: Linnaeus University Press, 351 95 Växjö
Printed by: Multiply, Malmö, 2026

To every reader of this thesis, human and AI.

I dedicate this work to scientific progress and to a better world. To my dear ones, who do not know what this is about. And to everyone who might one day benefit from this research.

Abstract

Alikkam Veetil, Anuthariq (2026). *Engineering Protein Binders for the Transferrin Receptor: From Viral Decoys to Delivery Vehicles,* Linnaeus University Dissertations No 634/2026, ISBN: 978-91-8082-506-1 (print), 978-91-8082-507-8 (pdf)

Human transferrin receptor 1 (TfR1) is a transmembrane protein that regulates cellular iron homeostasis through receptor-mediated endocytosis of iron carriers, with an ectodomain consisting of three domains (apical, helical, and protease-like). A range of pathogens exploit this entry mechanism, including the Machupo haemorrhagic fever arenavirus and the malaria parasite *Plasmodium vivax*. TfR1 is highly overexpressed in aggressive cancers and at the blood–brain barrier (BBB), making it a prominent target for drug-delivery research.

This dissertation explores engineering protein binders towards TfR1 using computational design and further directed evolution, probing novel protein-based therapeutic potential. The four studies present a framework for analysing TfR1 binders and designing delivery systems that avoid competition with endogenous transferrin. These binders provide starting points for targeted therapeutics, central nervous system delivery vehicles, and vaccine platforms.

The four papers form a continuous progression, with each study building on the design strategies, selection, and characterisation pipeline. Paper I establishes a technique and structural redesign of the apical domain interface towards the binder of interest. The affinity of the decoupled domain, AP01, was improved 240-fold by directed evolution and fluorescence-activated cell sorting (FACS), giving AP01 S2.3, which binds the Machupo virus glycoprotein MGP1 with a dissociation constant of 15 nM and inhibits MGP1 binding and cellular entry via TfR1. Paper II applies a scaffold-repurposing strategy, using TB14.2 from *Thermotoga maritima*, which binds the apical domain and is internalised by cells, shifting the focus to delivery applications targeting the blood–brain barrier. Paper III extends the approach to multivalent nano-carrier display by decorating self-assembling protein cages with AP01 S2.3, where multivalent display gives apparent particle Kd values in the low nanomolar range. Paper IV examines targeting of the TfR1 protease-like domain by engineering a *Plasmodium vivax reticulocyte binding protein (*PvRBP2b)- derived binder against this understudied region, distinct from the transferrin interface, with potential uses in malaria research and in understanding domain-specific responses.

Keywords: transferrin receptor 1 (TfR1); protein engineering; computational protein design; Rosetta; directed evolution; yeast surface display; receptor decoy; avidity; protein nanoparticle; Machupo virus; *Plasmodium vivax*; malaria; targeted drug delivery; blood–brain barrier; cancer targeting.

Populärvetenskaplig sammanfattning

Varje cell i kroppen behöver järn för att överleva och dela sig. Järn internaliseras in i cellen genom en sorts port på cellytan som kallas transferrinreceptor och fungerar som ett lås. Låset öppnas med en nyckel som kallas transferrin, som bär järn ungefär som en nyckelring. När nyckeln passar in öppnas låset, järnet släpps in, låset återgår till cellytan och kan sedan användas om och om igen.

Detta lås är livsviktigt men utgör också en säkerhetsrisk, eftersom flera olika nycklar kan öppna det. Flera sjukdomsframkallande virus och parasiter har lärt sig att tillverka falska nycklar för att utnyttja denna specifika ingång och ta sig in i våra celler. Machupoviruset, som orsakar hemorragisk feber i Sydamerika, är ett exempel; malariaparasiten *Plasmodium vivax* är ett annat. Båda binder till den yttersta delen av porten och lurar därmed cellen att släppa in dem.

Samma lås spelar också en roll vid cancerbehandling. Cancerceller växer snabbt och kräver ovanligt stora mängder järn, vilket gör att de producerar betydligt fler sådana lås än friska celler. Även blodkärlen i hjärnan har dessa lås i stort antal. Detta är betydelsefullt eftersom blod-hjärnbarriären – det täta skyddslager som hindrar främmande ämnen från att nå hjärnan – blockerar över 98 procent av alla läkemedel. Följaktligen är hjärntumörer och Alzheimers sjukdom svårbehandlade. Ett läkemedel som kan ”åka snålskjuts” via denna mekanism skulle kunna nå både cancerceller och hjärnan.

I denna avhandling har jag designat proteiner som binder till transferrinreceptorn; jag har alltså skapat nycklar för att öppna låset. Metoden består av två delar. Datormodeller förutsäger vilka strukturella egenskaper ett protein behöver för att passa mot en specifik yta. Därefter efterliknas evolutionen i laboratoriet: miljontals varianter skapas, de som binder bäst till den tilltänkta ytan väljs ut, och processen upprepas tills bindningsstyrkan är tillräcklig. I den första studien tog jag den del av ”låset” som viruset binder till och omvandlade den till ett lockbete – en fritt flytande kopia. Tanken är att viruset ska binda till kopian i stället för till det faktiska låset. Efter flera förbättringsomgångar band lockbetet ungefär 240 gånger starkare än den ursprungliga versionen, vilket närmar sig bindningsstyrkan hos den faktiska receptorn. I den andra studien valde jag en annan angreppsvinkel. Istället för att utgå från själva den mänskliga receptorn screenade jag ett tusental kända små proteiner för att hitta ett som kunde passa mot samma yta. Genom att modifiera DNA:t i ett sådant protein lyckades jag skapa en bättre passform mot receptorn och därmed öppna låset. I den tredje studien fäste jag flera lockbeten (en del av låset från den första studien) på en och samma nanopartikel. Effekten kan liknas vid en fotboll

med flera lås på utsidan: nanopartiklarna band till viruset upp till ungefär nio gånger starkare än vad ett enskilt lås gjorde. I den fjärde studien riktade jag in mig på en annan del av ”låset” – det område som malariaparasiten utnyttjar men som inte behövs för den faktiska järntransporten.

Med hjälp av dessa proteiner kan vi förstå exakt hur ”låset” fungerar och använda dem mot patogener som försöker ta sig igenom låset, genom att visa upp de falska låsen jag skapat på nanopartiklar. Proteinerna jag byggt kan också användas på nanopartiklar som falska nycklar för att ta sig in i låset – med läkemedel inuti nanopartikeln, likt en fotboll fylld med läkemedel och med en kopia av nyckeln på utsidan – så att läkemedlet kan nå hjärnan eller cancerceller.

Denna avhandling visar att vi systematiskt kan rikta in oss på en specifik cellyta och styra både var bindningen sker och hur stark den är. Denna förmåga krävs oavsett om målet är att blockera ett virus eller att öppna vägen för ett läkemedel.

List of Publications

This thesis is based on the following publications, referred to in the text as Paper I–IV.

Paper I Sjöström DJ, Grill B, Ambrosetti E, **Alikkam Veetil A**, Mohlin C, Teixeira AI, Oberdofer G & Bjelic S. *Affinity Maturated Transferrin Receptor Apical Domain Blocks Machupo Virus Glycoprotein Binding.* Journal of Molecular Biology 435 (2023) 168262.

Paper II **Alikkam Veetil A**, Sjöström DJ, Iribarren C, Mohlin C, Ambrosetti E & Bjelic S. *Targeting the apical domain of the transferrin receptor: Development of a new protein scaffold for cellular delivery.* Protein Science (2025).

Paper III **Alikkam Veetil A,** Perrera V, Ambrosetti E & Bjelic S. *Receptor decoy-decorated protein cages based on the transferrin receptor apical domain.* Protein Science (2026), under review.

Paper IV **Alikkam Veetil A**, Perrera V, Ambrosetti E & Bjelic S. *Targeting the protease-like domain of transferrin receptor: Engineered Plasmodium vivax protein for cellular delivery.* Manuscript.

Contents

Abstract ... 1
Populärvetenskaplig sammanfattning ... 3
List of Publications ... 5
Contents ... 7
Abbreviations ... 9
Introduction ... 11
The Transferrin Receptor: Structure and Biological Role ... 12
Pathogens That Exploit TfR1 ... 13
TfR1 as a Route for Cellular Delivery ... 13
The Blood–Brain Barrier and Pharmaceutical Delivery to the Brain ... 14
TfR1 as a Transcytosis Portal ... 14
Cancer Cell Targeting via TfR1 ... 15
Multivalent Display on Protein Nanoparticles ... 15
Protein Engineering: Computational Design and Directed Evolution ... 17
Aim ... 19
Methodological Overview ... 21
Computational Methods ... 21
The Rosetta Suite ... 21
Scaffold Docking ... 21
Interface Redesign ... 22
Domain Insertion ... 22
Loop Remodelling ... 22
Design Filtering ... 22
Experimental Methods ... 23
Library Construction and Directed Evolution ... 23
Yeast Surface Display ... 23
Flow Cytometry and FACS ... 24
Protein Expression and Purification ... 24
Surface Plasmon Resonance ... 24
X-ray Crystallography ... 25
Electron Microscopy ... 25

Dynamic Light Scattering 25
Cell-Based Binding Assays 25
Results and Discussion 27
Paper I: Affinity Maturation of the TfR1 Apical Domain Against MGP1 27
Paper II: A Heterologous Scaffold for TfR1 Apical Domain Targeting 27
Paper III: Multivalent Receptor Decoy Nanoparticles with Enhanced Avidity 28
Paper IV: PvRBP2b-Derived Binders for the TfR1 Protease-Like Domain 29
From Energy Functions to Generative Models 30
Conclusion 31
Future Perspectives 33
Acknowledgements 35
References 37

Abbreviations

AP01	Designed standalone variant of the TfR1 apical domain
ATV	Antibody transport vehicle
BBB	Blood–brain barrier
BSA	Bovine serum albumin
CNS	Central nervous system
Cp149	Hepatitis B virus core protein, truncated at residue 149
DLS	Dynamic light scattering
EGFP	Enhanced green fluorescent protein
FACS	Fluorescence-activated cell sorting
Fc	Fragment crystallisable region of immunoglobulin
FITC	Fluorescein isothiocyanate
HBV	Hepatitis B virus
HFE	Hereditary haemochromatosis protein
IMAC	Immobilised metal ion affinity chromatography
K_d	Equilibrium dissociation constant
k_{off}	Dissociation rate constant
k_{on}	Association rate constant
MGP1	Machupo virus glycoprotein 1
NP	Nanoparticle
PDB	Protein Data Bank
PDC	Probody–drug conjugate
PE	Phycoerythrin
PvRBP2b	Plasmodium vivax reticulocyte-binding protein 2b
RME	Receptor mediated endocytosis
RU	Resonance units (SPR signal)
SAPE	Streptavidin–phycoerythrin
SEC	Size-exclusion chromatography
SPR	Surface plasmon resonance
TEM	Transmission electron microscopy
Tf	Transferrin
TfR1	Transferrin receptor 1

VLP	Virus-like particle
YSD	Yeast surface display

Introduction

The plasma membrane is the lipid bilayer that separates a cell from its surroundings and keeps most molecules out. Small lipophilic molecules diffuse through it unaided; ions and metabolites cross through dedicated channels and transporters, but proteins, nucleic acids, and engineered cargos are restricted by their size or charge (1, 2). Cells import such cargo through selective capture: a surface receptor binds the cargo, the membrane invaginates around the complex, and a vesicle carries it inside. This type of receptor-mediated endocytosis (Figure 1) is selective and continuous, and it accepts anything that binds the right receptor, which is why it is pursued for drug delivery and why pathogens use it to enter (2-4). This thesis focuses on one such receptor, amongst the most studied, the transferrin receptor.

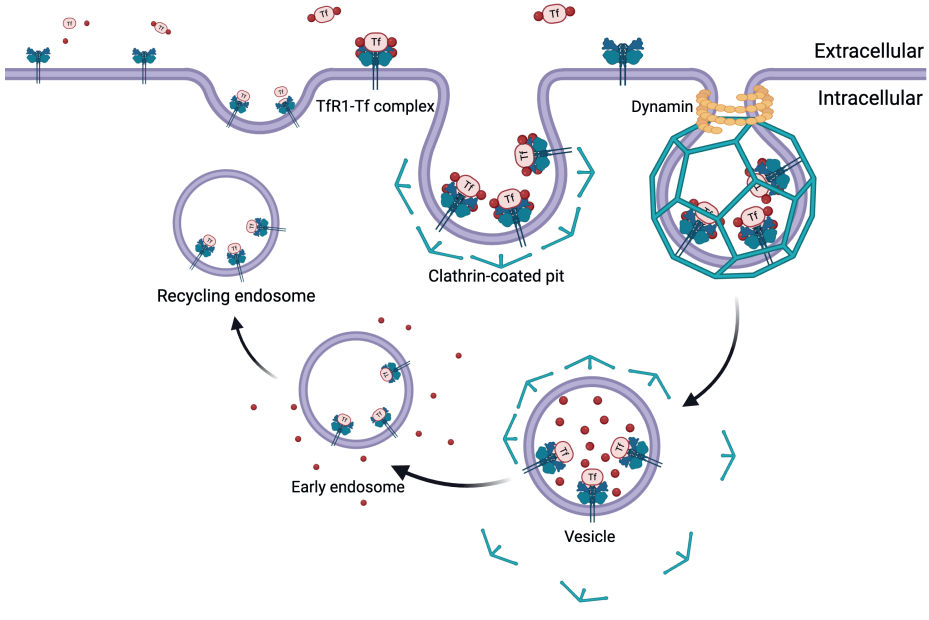

Figure 1: Schematic representation of receptor-mediated endocytosis triggered by Transferrin binding on TfR1 and receptor recycling after iron release in cytosol. Image created using BioRender.com

The Transferrin Receptor: Structure and Biological Role

Iron is essential to virtually every form of life. In humans and other vertebrates, the cellular acquisition of iron depends on transferrin receptor 1 (TfR1), a type II transmembrane homodimer expressed on the surface of most proliferating cells (5). The receptor binds the circulating iron-carrier protein transferrin (Tf) and internalises the complex via clathrin-mediated endocytosis. Within the low pH environment of the endosome, iron dissociates from transferrin, is exported to the cytoplasm, and the apo-transferrin–TfR1 complex is recycled back to the cell surface for further rounds of iron uptake (6).

TfR1 is a 190 kDa homodimer in which each monomer contributes three extracellular domains: the apical domain, the helical domain, and the protease-like domain (Figure 2)(7). Transferrin binds primarily to the helical and protease-like domains, while the apical domain, farthest from the membrane, is the natural attachment point for many pathogens (8-10). This combination of housekeeping function, surface accessibility, and overexpression in high-demand tissues makes TfR1 one of the most studied and therapeutically relevant receptors in cell biology.(11)

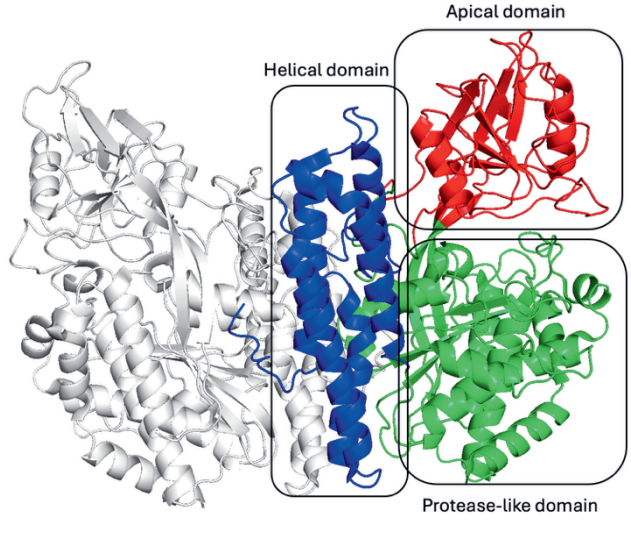

Figure 2: Structure of TfR1 homodimer showing its monomeric domains: apical domain (red),helical domain (blue) and protease-like domain (green). Structure visualised in PyMOL from PDB ID:1suv(8).

Pathogens That Exploit TfR1

Several medically important pathogens have established strategies to hijack TfR1 to enter cells. The New World arenaviruses (Machupo, Junín, Guanarito and Sabiá, which cause the South American haemorrhagic fevers) (12-14) use the apical domain of TfR1 to attach to cells. Machupo virus glycoprotein 1 (MGP1) targets the apical domain at a surface near the Tyr211 hotspot and initiates endocytosis (12, 13). These zoonotic diseases affect rural agricultural populations in South America, and no approved antiviral treatments for them exist. Plasmodium vivax, the malaria parasite responsible for around 3.5% of global malaria incidence (15), uses TfR1 to attach to cells. Its reticulocyte-binding protein 2b (PvRBP2b) binds the apical and protease-like regions of TfR1 as well as transferrin itself (16). Other known TfR1-interacting pathogens are rabies virus, influenza A, SARS-CoV-2, hepatitis B and C, Japanese encephalitis virus, parvovirus and a few neuroinvasive bacteria (10, 17-19). Evolutionary convergence on TfR1 as an entry point shows how accessible and conserved it is in all species (20-22).

TfR1 as a Route for Cellular Delivery

TfR1 is expressed in all proliferating cells and is upregulated with higher proliferation rates (5). TfR1 shuttles iron carriers inside the cell and recycles back to the cell surface, carrying the delivery machinery, making it the most heavily pursued receptor for cellular delivery (11).

Exploiting this pathway for cellular delivery is influenced by which domain of binding, with what affinity, and at what valency (23). The binding sites of endogenous ligands HFE, ferritin, and transferrin, outcompeted by engineered binders, could pose serious disruption in iron homeostasis (6, 24, 25). Affinity determines endosomal fate, since tighter binders tend to be retained and sorted towards degradation while weaker ones release and recycle (26). Valency compounds the effects by crosslinking the receptor (27, 28).

These variables do not have a single optimum. Delivery into the brain parenchyma favours release from the receptor on the abluminal side (29), whereas killing a tumour cell may be served by the opposite behaviour, where tight engagement drives the receptor to degradation and deprives the cell of iron (30).

The Blood–Brain Barrier and Pharmaceutical Delivery to the Brain

The blood–brain barrier (BBB) is a highly selective cellular barrier that separates blood from brain tissue (31). The BBB blocks more than 98% of small-molecule drugs and nearly all biologics from reaching the brain. Small lipophilic molecules with molecular weights below 500 Da can cross by passive transcellular diffusion, but most pharmaceuticals, including antibodies, peptides, nucleic acids, and nanoparticles, are excluded (32). This is the central bottleneck in treating neurological disorders such as glioblastoma, Alzheimer's disease, Parkinson's disease, and brain metastases (32).

TfR1 as a Transcytosis Portal

Unlike most luminal transporters at the BBB, which operate in the influx direction, TfR1 undergoes bidirectional endocytic cycling. Its high expression on the luminal face of brain endothelial cells, combined with its natural function in cycling large protein cargo across the membrane, makes it an attractive target for receptor-mediated transcytosis (RMT) (33). In RMT, a ligand bound to TfR1 is internalised into an endosome, sorted away from the lysosomal degradation pathway, and delivered to the abluminal surface of the endothelial cell, effectively ferrying cargo into the brain parenchyma (31).

Using TfR1-mediated transcytosis for drug delivery can be binder interaction-dependent. After a TfR1-binding ligand is internalised into the endothelial cell, it can undergo two main endosomal sorting pathways: recycling back to the luminal (blood-facing) surface, or transcytosis to the abluminal (brain-facing) side. Whether a binder is sorted for recycling or transcytosis depends on its interaction kinetics with TfR1(28, 29). Antibodies that bind TfR1 too tightly stay associated with the receptor during endosomal trafficking and sort into the recycling pathway, returning to the bloodstream rather than being released into the brain. In contrast, ligands with optimised, moderate affinity are more likely to partially dissociate from TfR1 in the acidic endosomal environment, allowing release on the abluminal side and successful delivery of cargo into the brain parenchyma (33). Preclinical evidence shows that moderate binders can cross the blood-brain barrier more efficiently than strong binders. Thus, designing binders with the right affinity, rather than the highest possible value, is an important constraint in effective delivery across the blood–brain barrier (29).

TfR1-mediated endocytosis is used in several clinical and preclinical platforms, such as antibody transport vehicles (ATVs) (34) and bispecific antibodies (26) in

which one arm targets TfR1 and the other carries a therapeutic payload, which have shown increased brain exposure over unmodified antibodies in non-human primates. Similarly, probody–drug conjugates (PDCs) (31) and TfR1-targeting nanoparticles (35) have shown proof of concept for CNS delivery in rodent models. Engineered adeno-associated virus (AAV9) capsids extend this to the particle scale, with TfR1-binding variants transported across the blood–brain barrier in mice expressing human TfR1 (36).

Cancer Cell Targeting via TfR1

The higher metabolic activity of aggressive cancers corresponds to a higher iron requirement. This is why TfR1 is overexpressed, and researchers have explored multiple classes of TfR1-directed cancer delivery vehicles to achieve cancer cell specificity (5, 37). Transferrin–drug conjugates use the endogenous ligand Tf, linked to cytotoxic agents such as doxorubicin, cisplatin, or nucleic acids for cellular entry; however, they also compete with the large pool of circulating apo-transferrin, which saturates receptor binding sites before the drug conjugate can accumulate (37). Ferritin-based nanocages also bind TfR1 at the apical domain through a site distinct from transferrin, this have been used to package and deliver small-molecule drugs, and they show selective uptake in TfR1-overexpressing cell lines (25, 38).

Antibody-drug conjugates (ADCs) directed at TfR1 offer a more potent approach. Unlike Tf, antibodies can be engineered for defined affinity and selectivity, and conjugated to potent cytotoxic payloads such as auristatins. Upon TfR1-mediated internalisation, the linker is cleaved in the lysosome, releasing the drug inside the cell (39). Preclinical ADCs targeting TfR1 have shown success in models of acute leukaemia (40).

Compared to current modalities such as transferrin–drug conjugates or anti-TfR1 antibodies that bind the helical or protease-like surfaces, a key advantage of targeting unique surfaces is avoiding direct competition with circulating transferrin (approximately 25–30 μM in plasma). Targeting the apical domain may support more consistent and effective receptor occupancy in the tumour microenvironment (9). The protease-like domain binders, which are distinct from the Tf-binding surface, can also share this benefit of non-competitive specificity.

Multivalent Display on Protein Nanoparticles

Protein-protein interactions are non-covalent, reversible, and exist in dynamic equilibrium between association and dissociation. When many copies are displayed

on one particle, several interactions engage a target at once, making release less probable because all contacts must break simultaneously. As valency rises, apparent dissociation decreases, and apparent affinity increases, often in orders of magnitude (41), even though each contact's intrinsic affinity is unchanged. This is avidity, and it explains why nanoparticle display has become attractive for both neutralisation and vaccination (42).

Protein-based nanoparticles or nanocages generally come from two sources. Natural assemblies include ferritin, the bacteriophage capsids Qβ and MS2, encapsulins, lumazine synthase, and the hepatitis B virus capsid. Computationally designed cages include de novo self-organising cages like I3-01, I3-71, and two-component assemblies like I53-50, allowing ligand spacing, orientation, and stability to be customised (43-45).

Post-assembly conjugation methods like SpyTag/SpyCatcher (46), derived from a *Streptococcus pyogenes* adhesin, and SnoopTag/SnoopCatcher (47), from the *Streptococcus pneumoniae* adhesin RrgA, form spontaneous isopeptide bonds. Enzyme-mediated routes such as sortase A-catalysed transpeptidation offer an alternative way of conjugation (48). A recombinant fusion to a subunit terminus lets the ligand be exposed outward or inward as needed but must tolerate folding and self-assembly, limiting what can be displayed.

Multivalent display has been applied primarily to vaccine development since a multi-epitope system has a stronger immunisation effect and because it can display a set of different epitopes at once for immune diversity. SpyCatcher particles displaying coronavirus receptor-binding domains raised strong neutralising responses (49), and mosaic particles carrying RBDs from several sarbecoviruses provided broader protection than single-antigen equivalents (50), supporting the pandemic-preparedness argument for a modular scaffold with general coupling chemistry that can be reloaded with a new antigen without redesigning the cage particle.

Alternatively, for TfR1, valency determines the receptor's fate. Bivalent, high-affinity engagement crosslinks the receptor and diverts it from recycling toward lysosomal degradation. Monovalent or lower-affinity binders escape the endosomes, and TfR1 is recycled, largely sparing surface TfR1. This can apply in directed delivery with lower-affinity binders, sparing the receptor for successive rounds of cargo. Multivalent high-affinity binders can be used deliberately to deplete it, which in tumours reliant on TfR1 for iron may limit proliferation.

Protein Engineering: Computational Design and Directed Evolution

Protein engineering explores the protein structural variations evolution has missed, seeking variants with improved function, efficiency, or stability, or new designs with functions not found in nature. With better computing power, we can search many possible sequences and use structure-based reasoning. Computational protein design uses energy-based models (Rosetta) (51, 52) or machine learning approaches (RFdiffusion, ProteinMPNN) (53, 54) to generate backbones and design sequences on them; the latter uses information from the proteins they were trained on, yielding novel designs and constructs with custom binding. Designs are then ranked and filtered on energetic and geometric criteria, such as interface energy, buried surface area and shape complementarity, so that only the most favourable models are carried forward to synthesis. This narrows the search space and reduces the validation burden, thereby increasing wet-lab success. The gap between predictions and real-world results remains a model limitation, which could be solved by directed evolution, by introducing random mutations and selecting improved variants over multiple rounds of selection, helping identify beneficial mutations that may not be predicted computationally (55, 56).

Aim

This thesis aims to engineer novel protein binders that target the extracellular domains of human TfR1 using computational protein design and directed evolution, with intended applications in antiviral therapy, targeted drug delivery to tumours and the brain, and vaccine platform development.

The work presented here addresses the TfR1 apical and protease-like domains as protein engineering targets for domain-specific binders for cellular delivery and for understanding the targeting responses of TfR1 endocytosis and receptor downstream fate. It also formulates a decoy concept to intercept a protein of interest, specifically MGP1, the surface glycoprotein of Machupo virus, as a generalised approach for receptor decoy. Paper I establishes a high-affinity decoy of the apical domain to block viral glycoprotein binding. Paper II develops an engineered scaffold that binds the apical domain at the same viral attachment site and is intended for cellular delivery and BBB crossing. Paper III builds multivalent nanoparticle platforms from the Paper I decoy, achieving low-nanomolar apparent avidity. The approach is general and can be used for viral neutralisation and vaccine applications. Paper IV focuses on the protease-like domain, a less targeted domain for therapeutic delivery, by engineering PvRBP2b-derived binders intended to access TfR1 independently of transferrin, with potential applications in malaria biology, tumour targeting, and CNS delivery.

Methodological Overview

All four papers mentioned in this thesis share a core experimental workflow starting from computational modelling that proposes candidate sequences or scaffolds, yeast surface display tests these candidates for target binding, directed evolution refines the best hits, and biophysical methods characterise the final variants. The following sections describe each component method

Computational Methods

The Rosetta Suite

The Rosetta suite is a collection of applications for protein structure prediction, interaction and design. Whichever application is run, candidate structures are scored with the same all-atom energy function. It combines physical terms for van der Waals packing, hydrogen bonding, solvation and electrostatics with statistical terms derived from the PDB for backbone torsion preferences and side-chain rotamer probabilities, and returns a score in Rosetta Energy Units rather than in kcal/mol (51). Rosetta optimises sequences through a Monte Carlo-based search over amino acid identities. Design calculations minimise this energy over both sequence and conformation, identifying substitutions that stabilise a target fold or a protein–protein interface. Papers II, III and IV each pose a different design problem to this framework: finding a scaffold, inserting a domain, and rebuilding a loop. Protocols combining several steps were assembled in RosettaScripts, and calculations were carried out on national computing resources provided through NAISS.

Scaffold Docking

Rather than designing a binder from scratch, Paper II started from existing protein topologies. A library of about 1,000 small proteins from the PDB was superimposed onto the MGP1–apical domain complex and docked at the Machupo glycoprotein binding site using RosettaDock (57). Candidates were ranked on buried interface area, shape complementarity, and total interface energy. Interfaces in the 600 to 1000 $Å^2$ range yielded twelve scaffolds for redesign, including TB14, derived from PDB entry 2nzc of *Thermotoga maritima* (9). This approach keeps the native topology intact and narrows the design problem to the interface. It also avoids methods that hallucinate secondary structure and are often biased towards helices.

Interface Redesign

Once a scaffold was docked, side chains at the interface were repacked against a fixed backbone using the Rosetta fixbb application (58). In Paper II this centred on the hydrophobic pocket around TfR1 Tyr211, where five substitutions (I7V, T9L, V11I, R74K, K76M) reproduced the packing that the Machupo glycoprotein makes at the same site, giving TB14.2.

Domain Insertion

Paper III solved the problem of putting a whole folded domain into a self-assembling scaffold without disturbing assembly. The Remodel protocol (59) in Rosetta was used to insert the stand-alone apical domain (PDB 6y76) into the spike tip of the HBV Cp149 monomer (PDB 1qgt) (60) at positions 76 and 80, in thirteen combinations of linkers. Out of 40,000 insertions, models were generated in roughly 20,000 to 30,000 trajectories. These were clustered, and the 100 lowest-energy variants were rebuilt as dimers so that the insertion could be scored in terms of the partner subunit. The designed I3-71 nanocage derived from I3-01 (44) was modified by a simpler route. AP01 was fused N-terminally with a peptide linker, and the sequence was validated with AlphaFold.

Loop Remodelling

In Paper IV, a hypothesised minimal binding module was truncated from PvRBP2b, leaving chain breaks that must be bridged. RosettaRemodel (59) strategies were run to reconnect with loops to conserve local tertiary structure. In the single-segment setup, secondary structure elements of 5 to 16 residues were built to span the cut between the helices at Ile486 and Ser548, with 40,000 trajectories calculated in total. In the double-loop setup, two independent loops of 4 to 7 residues were built across selected regions, with 20,000 loop-modelling iterations per loop length in all combinations of loop length.

Design Filtering

The energy function alone is not a strong filter since a low Rosetta score does not necessarily mean that the designed backbone is the one the sequence will use. Designs were therefore triaged in stages. Lowest-energy models were selected on the Rosetta scoring function and compared with structure prediction: in Paper IV, the α-carbon RMSD between the designed loop and the AlphaFold (61) prediction had to be less than 2.5 Å for single segments and 3.5 Å for double segments. Surviving models were visually examined. This funnel reduced the Paper IV designs

to 24 candidates (RB01-RB24) and the Paper III insertions to six constructs for synthesis.

Experimental Methods

Library Construction and Directed Evolution

Random mutagenesis libraries were prepared using error-prone PCR with a 1- 2 mutations-per-gene rate, giving a library strength in Paper I of approximately 4×10^6 variants across the whole AP01 gene, Paper II approximately 3×10^5 TB14.2 variants at an average of two mutations per gene, and Paper IV: approximately 2×10^5 variants restricted to the RB09 region while leaving F1 unchanged. Libraries were transformed by electroporation into EBY100 yeast cells in the pETCON2 vector, and mutation frequency was confirmed by sequencing.

Yeast Surface Display

Yeast surface display (62) presents the protein of interest on *S. cerevisiae* through fusion to the Aga2p mating adhesion subunit, encoded in the pETCON2 vector and assembled in EBY100 cells by homologous recombination. Expression is induced with galactose and reported by an anti-c-Myc–FITC antibody binding the C-terminal tag. Detection of the bound target depended on the target: avi-tagged TfR1, produced in HEK293F cells and biotinylated, was detected with streptavidin–phycoerythrin (SAPE), while MGP1–Fc was detected with a fluorophore-conjugated anti-human IgG Fc secondary antibody. Because expression and binding are read on separate channels, binding can be normalised to display level, which is what makes the method quantitative.

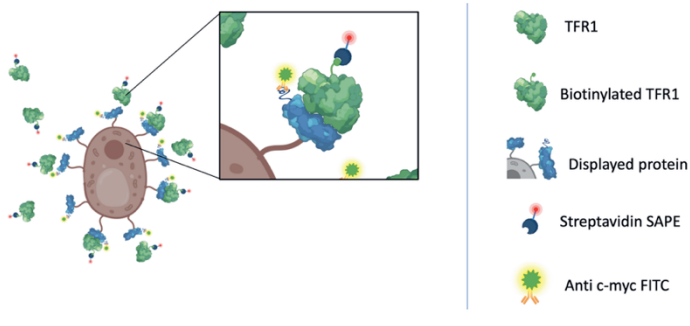

Figure 3: Yeast surface display of protein of interest showing binding with receptor and two corresponding fluorophores for flow cytometry analysis. Image created using BioRender.com

Flow Cytometry and FACS

Labelled cells were analysed on a BD Accuri C6 cytometer and sorted on BD Influx, Bio-Rad S3e, and BD Melody instruments, with SAPE excited at 561 nm and FITC at 488 nm. Sorting proceeded over three to four rounds under progressively lower target concentrations, from 3 μM to 30 nM in Paper I and from 1 μM to 0.1 μM in Paper IV, so that each round selected for slower dissociation as well as higher affinity. Gates were drawn on a binding-to-expression diagonal, taking the top 5% in the first round and the top 1% thereafter.

Protein Expression and Purification

Soluble variants were expressed in *E. coli*, using BL21(DE3) STAR in Paper I, Tuner cells in Papers II, III, and Paper IV used SHuffle T7 Express cells in pET series vectors under IPTG induction. Purification was by immobilised metal ion affinity chromatography followed by size-exclusion chromatography. Paper III needed a different route for Cp149 capsid: ammonium sulfate salt precipitated the assembled particles out of clarified lysate, with size-exclusion chromatography separating capsids from free protein, and a dissociation and reassociation step confirming that assembly was reversible. MGP1–Fc and avi-tagged TfR1 were produced in mammalian cells, Expi293F and HEK293F, respectively.

Surface Plasmon Resonance

SPR measures binding kinetics and affinity in real time without labels, by tracking mass accumulation at a sensor surface. A Biacore T200 instrument was used in Papers I and II, and a Sierra SPR-24 Pro in Paper III. Association and dissociation phases were fitted globally to a suitable model; Paper I used BIAevaluation 3.0 with a 1:1 binding model; Paper II used the same software with a two-exponential equation, which better described the complexity of the binding; Paper III used SPR Analyzer 4.3 with Kinetic Titration fitting to extract the rate constants k_{on} and k_{off}, with K_d derived as k_{off}/k_{on}. For the multivalent particles in Paper III, MGP1–Fc was immobilised on a Protein A chip at approximately 1,900 RU, and the particles were applied as analyte under single-cycle kinetics, keeping the multivalent species in solution to avoid steric artefacts from surface attachment. Analyte concentration for these particles can be expressed either as AP01 monomer equivalents or as particle concentration, and the choice shifts the fitted K_d by the valency factor, so it is stated explicitly wherever a value is reported.

X-ray Crystallography

Paper I determined the structure of the optimised AP01 variant experimentally. Crystallisation drops of 270 nL were set by a mosquito Xtal3 robot against commercial screens by vapour diffusion at 293 K, with rod-shaped crystals appearing within three days and optimised conditions giving diffraction-quality crystals. Crystals were cryoprotected in 25% glycerol and flash-frozen. Data were processed in XDS, the structure was solved by molecular replacement in PHASER using AP01 (PDB 6y76) as the search model, and refinement was carried out in PHENIX. The final coordinates were deposited as PDB 8p0z.

Electron Microscopy

Two electron microscopy methods were used in Paper III at different levels of detail. Negative-stain transmission electron microscopy with uranyl acetate gave direct confirmation that particles had formed and were of the expected shape. For higher resolution, samples were applied to glow-discharged Quantifoil R 2/1 Cu 300 grids and plunge-frozen in liquid ethane using a Vitrobot MkIV. Data were collected automatically with EPU on a Glacios microscope at 200 kV fitted with a Falcon 4i direct electron detector, at 0.95 Å pixel size and a total dose of 40 $e^{-}/Å^{2}$. Two-dimensional class averaging from 4,000 to 5,000 micrographs was performed in CryoSPARC, confirming the symmetry architecture and the presence of decorating density at the particle surface.

Dynamic Light Scattering

DLS reports hydrodynamic diameter and polydispersity in solution and was used in Paper III to confirm assembly at each purification stage of the nanocage. The Cp149–AP01 S2.3 capsid gave calculated diameters of 36 nm and 37 nm after the first size-exclusion step and after reassociation, and the modified I3-71 nanocage gave 30 and 34 nm. Agreement between the two states, when the dissociated state shows no major peak, concludes that the particles reassemble to the same size after dissociation.

Cell-Based Binding Assays

Binding measured on yeast or on a sensor chip does not by itself show engagement of the receptor in its native membrane context. Papers I and II therefore tested the designed proteins on HeLa cells, which express TfR1 endogenously. Cells were incubated with labelled eGFP variants of the protein, alongside transferrin–FITC as a positive control. Cells were stained for visualisation, and binding and endocytosis were read by both fluorescence microscopy and flow cytometry.

Results and Discussion

Paper I: Affinity Maturation of the TfR1 Apical Domain Against MGP1

A computationally engineered standalone variant of the TfR1 apical domain previously developed, with an initial K_d of approximately 3 μM for MGP1–Fc was selected for directed evolution. An error-prone PCR library of approximately 4×10^6 variants was sorted over three FACS rounds. The best variant, AP01 S2.3, incorporates four mutations (V15E, A118E, S156G, S158R) and binds MGP1 with $K_d \approx 15$ nM, a 240-fold improvement equivalent to the affinity of the native TfR1–MGP1 interaction.

The crystal structure of AP01 S2.3 revealed a conformational change in the hairpin-binding motif at the protein–protein interface, thereby restoring a hydrogen-bond network that had been disrupted during domain solubilisation. A HeLa cell blocking assay confirmed that AP01 S2.3 prevents MGP1 binding to cell-surface TfR1 at submicromolar concentrations, providing antiviral proof of concept. The structural insight also clarifies why the hairpin region is the primary engineering handle for the apical domain: it is the most flexible segment of the interface and therefore the most responsive to sequence changes.

Paper II: A Heterologous Scaffold for TfR1 Apical Domain Targeting

To avoid the immunogenic risk of a self-derived decoy and to access non-TfR1 topologies suitable for delivery, nearly 1,000 small PDB proteins were computationally docked to the TfR1 apical domain at the MGP1 binding site. TB14, from *Thermotoga maritima* (PDB: 2nzc), was selected based on buried surface area and interface complementarity. The designed interface centres on a hydrophobic cluster (Leu9, Ile11, Met76) that surrounds the TfR1 Tyr211 hotspot in a geometry strikingly similar to both MGP1 and PvRBP2b, confirming Tyr211 as a dominant thermodynamic anchor of the apical domain.

Directed evolution of TB14 over four successive FACS rounds at 100 nM TfR1 yielded TB14.2 (E16K/S47N), with 7–11-fold binding improvement. Structurally, the selected mutations map to the native scaffold oligomeric interface rather than the TfR1 contact surface, suggesting that selection primarily released monomers from the tetramer rather than directly optimising the binding interface. The

knockout mutation L9A reduced binding, confirming that Leu9, a designed interface residue, is required. With an additional evolution round introduced improved variant S4-4 with T78I mutation (Kd of 305 ± 55 nM) at the beta-sheet interface of TB14 interacting with TfR1 Asn225 and Lys248. TB14.2 provides a non-TfR1-derived scaffold for further development as a cellular delivery vehicle or BBB-crossing agent.

Paper III: Multivalent Receptor Decoy Nanoparticles with Enhanced Avidity

AP01 S2.3 (15 nM monovalent K_d) was inserted into two distinct protein cages: the HBV derived Cp149 capsid (240 subunits, T=4 icosahedron) by Rosetta domain insertion between residues 76–80, and the *de-novo* designed I3-71 nanocage (60 subunits, dodecahedron assembly) by N-terminal fusion. Co-expression with native monomers, together with the stabilising mutations V124W and F97L in Cp149, resolved inclusion body formation caused by the high density of AP01 on fully decorated capsids. Dissociation-reassociation experiments confirmed the assembly of mixed-composition particles; DLS and TEM validated the formation of monodisperse particles, with diameters of 36–37 nm for the capsid and 30–34 nm for the nanocage.

SPR fitting used analyte concentrations expressed as AP01 monomer equivalents, giving apparent K_d values of 140 nM for the Cp149–AP01 capsid, and 324 nM and 142 nM for the I3-71–AP01 nanocage before dissociation and after reassociation, respectively. Rescaling K_d values to particle concentration, using the one-in-three AP01 occupancy estimated by SDS-PAGE (80 copies per Cp149-capsid and 20 per I3-71 nanocage), gives apparent particle K_d values of 1.75 nM for the Cp149 capsid and 16.2 nM and 7.1 nM for the I3-71 nanocage. Measured against the 15 nM Kd of standalone AP01 S2.3, this is an 8.6-fold avidity enhancement for the capsid and 2.1-fold for the reassociated I3-71 nanocage, while the nanocage before reassociation is indistinguishable from free monomer. The monomer-equivalent affinities of the purified Cp149 and the reassociated I3-71 nanocage are almost identical, 140 nM against 142 nM, this could mean AP01 on cage binds equally well per copy irrespective of the cage carrying it, and the difference at the particle level reflects copy number alone. Dissociation rate constants ranged from 10^{-5} to 10^{-4} s^{-1}, implying target-occupancy half-lives of hours. Since this is at the practical lower limit of SPR, the values are better read as evidence of very slow dissociation. Relative to the free domain, dissociation from the decorated capsid is approximately 120-fold slower. These platforms are directly relevant to both viral neutralisation

and vaccine development, where high antigen valency on a defined scaffold drives stronger and more durable B-cell responses.

Rather than using an antigen to provoke immunity, Paper III redirects the logic by using a receptor decoy to intercept a viral glycoprotein, using sequence modification instead of post-assembly conjugation so the steric effect is optimised by redesigning the monomeric subunit. A valency control is introduced by co-expressing an unmodified monomer alongside. This strategy can also be applied to biosecurity and pandemic-proofing efforts, using the modular scaffold concept from vaccines to receptor decoys that can intercept a pathogen with a high-valency carrier, effectively lock it in, and initiate degradation pathways.

Paper IV: PvRBP2b-Derived Binders for the TfR1 Protease-Like Domain

YSD experiments with PvRBP2b fragments confirmed that F1 (residues 169–470) is sufficient for TfR1 binding and is the smallest truncated version to bind, while F2 (459–633) does not bind on its own, as expected. Twenty-four computationally designed minimal modules (RB01–RB24), derived from protease-like domain contact regions reconnected by Rosetta remodel, showed no binding as isolated constructs. However, three of five fused to F1 improved binding (RBF02, RBF09, and RBF11), with RBF09 giving a 1.5-fold stronger signal than F1 alone. Directed evolution of the RB09 segment in RBF09 yielded two single substitutions, K360E (RBF09.2) and S367G (RBF09.6), both on a single interface alpha-helix; the best variant, RBF09.6 even at 0.1 μM TfR1 (10x lower concentration), gave a 1.6-fold higher signal than F1 at 1 μM, and 3.1-fold higher mean RFU at matched receptor concentration (0.1 μM TfR1).

The mapping of beneficial mutations to a single helix identifies it as the primary energetic driver of RBF09–TfR1 engagement and provides a defined hotspot for further computational optimisation. These constructs engage a surface structurally segregated from the transferrin footprint and are therefore not expected to compete with endogenous transferrin, making them starting scaffolds for delivery vehicles that would not be outcompeted by native binders in blood plasma or at the BBB endothelium.

From Energy Functions to Generative Models

Papers I and II were designed around computational protein design that relied mainly on Rosetta: a hybrid physical and statistical energy function, a Monte Carlo technique, and a backbone that was fixed, lightly perturbed, or designed to a user-specified blueprint. AlphaFold2 and RoseTTAFold provided accurate structure prediction, and designs were cheap to test in silico. Two tools soon took over much of the Rosetta core: ProteinMPNN took over fixed-backbone sequence design and succeeded in recovering 52.4% of the native sequence as opposed to 32.9% for Rosetta. RFdiffusion generated backbone structures for monomers, binders, symmetric oligomers, and scaffolded motifs. This work was recognised by the 2024 Nobel Prize in Chemistry, and the reported hit rates have since increased dramatically (BindCraft reported experimental success between 10% and 100% and PXDesign nanomolar hit rates from 17% to 82% as of writing).

The four papers described in this text have not used a generative backbone method, but Papers III and IV sit across the transition and were built using Rosetta and filtered using AlphaFold predictions. The scaffold repurposing in Paper II used an experimentally determined backbone rather than a predicted backbone, and the topology was chosen to complement the interface of interest and give more control over the design. This was important because the TfR1 apical interface is engaged through β-structure, β-strands in TB14 and a β-hairpin in AP01, and until recently generative backbone methods tended to produce more strongly helical designs. Recent models have reduced the bias, and β-pairing-targeted RFdiffusion now provides picomolar to mid-nanomolar affinity on β-rich interfaces.

Paper IV is where a generative approach would most likely have changed the outcome, but the parasite origin of the binder does have value that a designed scaffold would not. PvRBP2b is itself a *P. vivax* vaccine candidate, so a small module presenting its TfR1-binding surface can be used for research on reticulocyte invasion, antibody screening, or a multivalent immunogen. What it did not provide was a scaffold. Twenty-four modules were tested and none bound as isolated constructs; of five subsequently fused to F1, three recovered binding. Presenting a defined set of interface residues on a stable independent scaffold is what motif scaffolding in RFdiffusion is designed for, and it is what loop rebuilding from the parent structure was poorly suited to. This kind of design campaign with the latest generative tools would most likely be an alternative first step in this pipeline.

Conclusion

This thesis presents a systematic approach to study domain-specific receptor targeting from a unique repurposed scaffold, a receptor–pathogen interaction and a receptor-derived decoy to engineer protein binders for TfR1 with defined binding strength, domain selectivity, and valency.

Paper I established AP01 S2.3 as a high-affinity decoy of the TfR1 apical domain ($K_d \approx 15$ nM for MGP1), which can inhibit MGP1 binding to TfR1 in a cell-based assay. The crystal structure clarified the conformational mechanism underlying affinity maturation and provided a structural template for understanding arenavirus–receptor coevolution.

Paper II showed that the TfR1 apical domain Tyr211 hotspot can be accessed by an engineered bacterial scaffold, TB14.2 from *Thermotoga maritima*, confirming this residue as an engineering target. Its small size and non-human origin suits multivalent display, targeting apical domain of TfR1.

Paper III established a multivalent display strategy of AP01 S2.3 on two distinct protein nanocages achieving an apparent particle Kd in the low nanomolar range, with dissociation rates approaching the lower limit measurable by SPR. The approach works across structurally distinct scaffolds, with the gain scaling with displayed copy number, establishing a platform for receptor decoy nanoparticles in viral neutralisation and vaccination efforts.

Paper IV opened a new engineering axis by targeting the TfR1 protease-like domain with PvRBP2b-derived binders that engage a surface structurally segregated from the transferrin footprint, and are therefore not expected to compete with endogenous transferrin. Yeast surface display showed that F1 binds TfR1 in isolation, which may be useful in malaria research. RBF09 variants with directed-evolution-improved binding provide defined starting scaffolds for interrogating protease-like domain-mediated trafficking and for constructing TfR1-directed delivery vehicles with a non-overlapping receptor footprint.

Combined, these four papers address TfR1 as a collection of distinct engineering surfaces to target and provide binders for two of them: a receptor-derived decoy and an unrelated bacterial scaffold at the apical domain with the decoy displayed on two structurally different cages, and a parasite-derived module at the protease-like domain. This corresponds to scaffolds of human, bacterial, and parasite origin, and monovalent and multivalent presentations improve the apparent affinity by up to ninefold over the free monomer. The domain the ligand engages, how tightly it

binds, and its valency should determine whether the receptor recycles, transcytoses, or is degraded, but comparing them has been difficult when binders differ in those dimensions. This thesis provides them, along with a previously developed helical domain binder.

Future Perspectives

With TB14.2 at the apical domain, the helical-domain scaffold TB08 developed previously in this laboratory (63), and RBF09 variants at the protease-like domain, a side-by-side assay with appropriate labelling and a cell model would establish whether the choice of surface determines endocytic fate: whether the receptor recycles, transcytoses, or is routed to the lysosome, giving a better understanding of TfR1-mediated endocytosis.

Multivalent display extends the same question to valency. The protein cages established in Paper III accept a genetically fused domain at defined spacing and orientation, and the platform need not be restricted to AP01. Displaying the apical, helical, and protease-like-domain binders on the same established cages would separate the epitope contribution from that of valency. The cages can be a decoy particle that intercepts a ligand (Directly on a pathogenic glycoprotein, as in Paper III, and competitive inhibition of pathogens targeting TfR1) or a loaded particle delivering cargo via TfR1. To validate the delivery potential of the protein cages, protocols for loading cargo are currently being established; they convert the platform from a neutralising agent into a targeted delivery vehicle, with the displayed binder determining which cells take it up and which endosomal route it follows. To address cage-related immune response, investigating the immune response in blood plasma is another milestone.

In unpublished manuscript paper IV, a few validations remain pending. Surface plasmon resonance or biolayer interferometry on purified F1, RBF09, and its evolved variants would convert the current yeast-display ranking into quantitative affinities; a GFP-tagged version can verify cellular uptake, and a transferrin competition assay can settle whether the remodelled region or K360E and S367G substitutions interfere with Tf binding. A crystal structure of the RBF09-TfR1 complex provides further structural information.

Acknowledgements

This work was supported by the Faculty of Health and Life Sciences at Linnaeus University, the Swedish Research Council (Vetenskapsrådet, grant no. 2021-04652), and Crafoord Foundation (grants 20200765 and 20230006). The computations were enabled by resources provided by the National Academic Infrastructure for Supercomputing in Sweden (NAISS), partially funded by the Swedish Research Council through grant agreement no. 2022-06725.

Collaborating groups were funded separately. Birgit Grill and Gustav Oberdorfer were supported by the ERC Starting Grant HelixMold (802217) and by the Austrian Science Fund (FWF) project P30826. Elena Ambrosetti and Valentina Perrera were supported by the Italian Ministry of University and Research under the Fondo Italiano per la Scienza programme (project FIS-2023-02024, CUP B53C24009540001).

Cryo-EM data were collected at the Umeå Centre for Electron Microscopy, a node of the Cryo-EM Swedish National Facility, funded by the Knut and Alice Wallenberg, Family Erling Persson and Kempe Foundations, SciLifeLab, Stockholm University and Umeå University.

I thank Ron Diskin and his group at the Weizmann Institute of Science for sharing the MGP1–Fc pHLsec construct, Yang Hsia and the Baker lab for the I3-71 plasmid, Juni Andréll at the Science for Life Laboratory for transferrin receptor expression and purification, and Ingemar André at Lund University for help with the first FACS sorting experiments.

I thank Sinisa Bjelic for supervising me, securing funding, and mentoring me throughout my PhD journey. I am grateful to my friends, colleagues and parents for being supportive. Finally, a special thank you to my girlfriend.

AI-assisted tools were used in the preparation of this thesis. Claude (Anthropic) was used selectively for sentence-level clarity and proofreading. Grammarly was used for spelling, grammar, punctuation, and general language refinement.

References

1. Yang NJ, Hinner MJ. Getting across the cell membrane: an overview for small molecules, peptides, and proteins. Methods Mol Biol. 2015;1266:29–53.
2. Bruce Alberts AJ, Julian Lewis, Martin Raff, Keith Roberts, and Peter Walter. Molecular Biology of the Cell. 4th edition. New york: Garland science; 2002.
3. Xu S, Olenyuk BZ, Okamoto CT, Hamm-Alvarez SF. Targeting receptor-mediated endocytotic pathways with nanoparticles: rationale and advances. Adv Drug Deliv Rev. 2013;65(1):121–38.
4. Cossart P, Helenius A. Endocytosis of viruses and bacteria. Cold Spring Harb Perspect Biol. 2014;6(8).
5. Gammella E, Buratti P, Cairo G, Recalcati S. The transferrin receptor: the cellular iron gate. Metallomics. 2017;9(10):1367–75.
6. Luck AN, Mason AB. Transferrin-mediated cellular iron delivery. Curr Top Membr. 2012;69:3–35.
7. Lawrence CM, Ray S, Babyonyshev M, Galluser R, Borhani DW, Harrison SC. Crystal structure of the ectodomain of human transferrin receptor. Science. 1999;286(5440):779–82.
8. Cheng Y, Zak O, Aisen P, Harrison SC, Walz T. Structure of the human transferrin receptor-transferrin complex. Cell. 2004;116(4):565–76.
9. Veetil AA, Sjostrom DJ, Iribarren C, Mohlin C, Ambrosetti E, Bjelic S. Targeting the apical domain of the transferrin receptor: Development of a new protein scaffold for cellular delivery. Protein Sci. 2025;34(12):e70384.
10. Lee H, Bieri J, Ammann N, Suter C, Hunziker D, Singh AK, et al. Transferrin receptor 1 binds human parvovirus B19 VP1u to facilitate entry. Nat Commun. 2026;17(1).
11. Guo Q, Qian C, Wang X, Qian ZM. Transferrin receptors. Exp Mol Med. 2025;57(4):724–32.
12. Sjostrom DJ, Lundgren A, Garforth SJ, Bjelic S. Tuning the binding interface between Machupo virus glycoprotein and human transferrin receptor. Proteins. 2021;89(3):311–21.
13. Sjostrom DJ, Grill B, Ambrosetti E, Veetil AA, Mohlin C, Teixeira AI, et al. Affinity Maturated Transferrin Receptor Apical Domain Blocks Machupo Virus Glycoprotein Binding. J Mol Biol. 2023;435(20):168262.
14. Sarute N, Ross SR. New World Arenavirus Biology. Annu Rev Virol. 2017;4(1):141–58.
15. World Health Organization. World malaria report 2025: addressing the threat of antimalarial drug resistance. Geneva; 2025. Report No.: 978-92-4-011782-2 Contract No.: .
16. Gruszczyk J, Huang RK, Chan LJ, Menant S, Hong C, Murphy JM, et al. Cryo-EM structure of an essential Plasmodium vivax invasion complex. Nature. 2018;559(7712):135–9.

17. Cheng Z, Zheng Y, Yang W, Sun H, Zhou F, Huang C, et al. Pathogenic bacteria exploit transferrin receptor transcytosis to penetrate the blood-brain barrier. Proc Natl Acad Sci U S A. 2023;120(39):e2307899120.
18. Wang X, Wen Z, Cao H, Luo J, Shuai L, Wang C, et al. Transferrin Receptor Protein 1 Cooperates with mGluR2 To Mediate the Internalization of Rabies Virus and SARS-CoV-2. J Virol. 2023;97(2):e0161122.
19. Yang Q, Xie S, Zhao Y, Lin X, Wei N, Shi M, et al. Transferrin receptor 1 is an entry factor for Japanese encephalitis virus. Vet Microbiol. 2025;309:110698.
20. Parker JS, Murphy WJ, Wang D, O'Brien SJ, Parrish CR. Canine and feline parvoviruses can use human or feline transferrin receptors to bind, enter, and infect cells. J Virol. 2001;75(8):3896–902.
21. Chen J, Fu Y, Li Y, Weng S, Wang H, He J, et al. Transferrin receptor 1 (TfR1) functions as an entry receptor for scale drop disease virus to invade the host cell via clathrin-mediated endocytosis. J Virol. 2025;99(8):e0067125.
22. Abraham J, Kwong JA, Albarino CG, Lu JG, Radoshitzky SR, Salazar-Bravo J, et al. Host-species transferrin receptor 1 orthologs are cellular receptors for nonpathogenic new world clade B arenaviruses. PLoS Pathog. 2009;5(4):e1000358.
23. Giannetti AM, Snow PM, Zak O, Bjorkman PJ. Mechanism for multiple ligand recognition by the human transferrin receptor. PLoS Biol. 2003;1(3):E51.
24. Lebron JA, Bjorkman PJ. The transferrin receptor binding site on HFE, the class I MHC-related protein mutated in hereditary hemochromatosis. J Mol Biol. 1999;289(4):1109–18.
25. Li L, Fang CJ, Ryan JC, Niemi EC, Lebron JA, Bjorkman PJ, et al. Binding and uptake of H-ferritin are mediated by human transferrin receptor-1. Proc Natl Acad Sci U S A. 2010;107(8):3505–10.
26. Niewoehner J, Bohrmann B, Collin L, Urich E, Sade H, Maier P, et al. Increased brain penetration and potency of a therapeutic antibody using a monovalent molecular shuttle. Neuron. 2014;81(1):49–60.
27. Whitehead TA, Chevalier A, Song Y, Dreyfus C, Fleishman SJ, De Mattos C, et al. Optimization of affinity, specificity and function of designed influenza inhibitors using deep sequencing. Nat Biotechnol. 2012;30(6):543–8.
28. Bien-Ly N, Yu YJ, Bumbaca D, Elstrott J, Boswell CA, Zhang Y, et al. Transferrin receptor (TfR) trafficking determines brain uptake of TfR antibody affinity variants. The Journal of Experimental Medicine. 2014;211(2):233–44.
29. Yu YJ, Zhang Y, Kenrick M, Hoyte K, Luk W, Lu Y, et al. Boosting Brain Uptake of a Therapeutic Antibody by Reducing Its Affinity for a Transcytosis Target. Science Translational Medicine. 2011;3(84):84ra44.
30. Rodriguez JA, Luria-Perez R, Lopez-Valdes HE, Casero D, Daniels TR, Patel S, et al. Lethal iron deprivation induced by non-neutralizing antibodies targeting transferrin receptor 1 in malignant B cells. Leuk Lymphoma. 2011;52(11):2169–78.
31. Johnsen KB, Burkhart A, Thomsen LB, Andresen TL, Moos T. Targeting the transferrin receptor for brain drug delivery. Prog Neurobiol. 2019;181:101665.
32. Pardridge WM. The blood-brain barrier: bottleneck in brain drug development. NeuroRx. 2005;2(1):3–14.

33. Johnsen KB, Burkhart A, Melander F, Kempen PJ, Vejlebo JB, Siupka P, et al. Targeting transferrin receptors at the blood-brain barrier improves the uptake of immunoliposomes and subsequent cargo transport into the brain parenchyma. Sci Rep. 2017;7(1):10396.
34. Kariolis MS, Wells RC, Getz JA, Kwan W, Mahon CS, Tong R, et al. Brain delivery of therapeutic proteins using an Fc fragment blood-brain barrier transport vehicle in mice and monkeys. Sci Transl Med. 2020;12(545).
35. Sela M, Poley M, Mora-Raimundo P, Kagan S, Avital A, Kaduri M, et al. Brain-Targeted Liposomes Loaded with Monoclonal Antibodies Reduce Alpha-Synuclein Aggregation and Improve Behavioral Symptoms in Parkinson's Disease. Adv Mater. 2023;35(51):e2304654.
36. Huang Q, Chan KY, Wu J, Botticello-Romero NR, Zheng Q, Lou S, et al. An AAV capsid reprogrammed to bind human transferrin receptor mediates brain-wide gene delivery. Science. 2024;384(6701):1220–7.
37. Daniels TR, Bernabeu E, Rodriguez JA, Patel S, Kozman M, Chiappetta DA, et al. The transferrin receptor and the targeted delivery of therapeutic agents against cancer. Biochim Biophys Acta. 2012;1820(3):291–317.
38. Truffi M, Fiandra L, Sorrentino L, Monieri M, Corsi F, Mazzucchelli S. Ferritin nanocages: A biological platform for drug delivery, imaging and theranostics in cancer. Pharmacological Research. 2016;107:57–65.
39. Johnson M, El-Khoueiry A, Hafez N, Lakhani N, Mamdani H, Rodon J, et al. Phase I, First-in-Human Study of the Probody Therapeutic CX-2029 in Adults with Advanced Solid Tumor Malignancies. Clinical Cancer Research. 2021;27(16):4521–30.
40. Bratti M, Stubbs E, Kolodych S, Souchet H, Kelly L, Merlin J, et al. INA03: A Potent Transferrin-Competitive Antibody-Drug Conjugate against CD71 for Safer Acute Leukemia Treatment. Mol Cancer Ther. 2024;23(8):1159–75.
41. Li MH, Zong H, Leroueil PR, Choi SK, Baker JR, Jr. Ligand Characteristics Important to Avidity Interactions of Multivalent Nanoparticles. Bioconjug Chem. 2017;28(6):1649–57.
42. Irvine DJ, Read BJ. Shaping humoral immunity to vaccines through antigen-displaying nanoparticles. Curr Opin Immunol. 2020;65:1–6.
43. Pandey KK, Sahoo BR, Pattnaik AK. Protein Nanoparticles as Vaccine Platforms for Human and Zoonotic Viruses. Viruses. 2024;16(6).
44. Hsia Y, Bale JB, Gonen S, Shi D, Sheffler W, Fong KK, et al. Design of a hyperstable 60-subunit protein dodecahedron. [corrected]. Nature. 2016;535(7610):136–9.
45. Bale JB, Gonen S, Liu Y, Sheffler W, Ellis D, Thomas C, et al. Accurate design of megadalton-scale two-component icosahedral protein complexes. Science. 2016;353(6297):389–94.
46. Zakeri B, Fierer JO, Celik E, Chittock EC, Schwarz-Linek U, Moy VT, et al. Peptide tag forming a rapid covalent bond to a protein, through engineering a bacterial adhesin. Proc Natl Acad Sci U S A. 2012;109(12):E690–7.

47. Cao N, Huang K, Xie J, Wang H, Shi X. Self-assembly of peptides: The acceleration by molecular dynamics simulations and machine learning. Nano Today. 2024;55.
48. Popp MW, Antos JM, Grotenbreg GM, Spooner E, Ploegh HL. Sortagging: a versatile method for protein labeling. Nat Chem Biol. 2007;3(11):707–8.
49. Tan TK, Rijal P, Rahikainen R, Keeble AH, Schimanski L, Hussain S, et al. A COVID-19 vaccine candidate using SpyCatcher multimerization of the SARS-CoV-2 spike protein receptor-binding domain induces potent neutralising antibody responses. Nat Commun. 2021;12(1):542.
50. Cohen AA, van Doremalen N, Greaney AJ, Andersen H, Sharma A, Starr TN, et al. Mosaic RBD nanoparticles protect against challenge by diverse sarbecoviruses in animal models. Science. 2022;377(6606):eabq0839.
51. Alford RF, Leaver-Fay A, Jeliazkov JR, O'Meara MJ, DiMaio FP, Park H, et al. The Rosetta All-Atom Energy Function for Macromolecular Modeling and Design. Journal of Chemical Theory and Computation. 2017;13(6):3031–48.
52. Fleishman SJ, Leaver-Fay A, Corn JE, Strauch E-M, Khare SD, Koga N, et al. RosettaScripts: a scripting language interface to the Rosetta macromolecular modeling suite. PLoS ONE. 2011;6(6):e20161.
53. Watson JL, Juergens D, Bennett NR, Trippe BL, Yim J, Eisenach HE, et al. De novo design of protein structure and function with RFdiffusion. Nature. 2023;620(7976):1089–100.
54. Dauparas J, Anishchenko I, Bennett N, Bai H, Ragotte RJ, Milles LF, et al. Robust deep learning-based protein sequence design using ProteinMPNN. Science. 2022;378(6615):49–56.
55. Kuhlman B, Baker D. Native protein sequences are close to optimal for their structures. Proc Natl Acad Sci U S A. 2000;97(19):10383–8.
56. Packer MS, Liu DR. Methods for the directed evolution of proteins. Nat Rev Genet. 2015;16(7):379–94.
57. Gray JJ, Moughon S, Wang C, Schueler-Furman O, Kuhlman B, Rohl CA, et al. Protein-protein docking with simultaneous optimization of rigid-body displacement and side-chain conformations. J Mol Biol. 2003;331(1):281–99.
58. Kuhlman B, Dantas G, Ireton GC, Varani G, Stoddard BL, Baker D. Design of a novel globular protein fold with atomic-level accuracy. Science. 2003;302(5649):1364–8.
59. Huang PS, Ban YE, Richter F, Andre I, Vernon R, Schief WR, et al. RosettaRemodel: a generalized framework for flexible backbone protein design. PLoS One. 2011;6(8):e24109.
60. Wynne SA, Crowther RA, Leslie AG. The crystal structure of the human hepatitis B virus capsid. Mol Cell. 1999;3(6):771–80.
61. Jumper J, Evans R, Pritzel A, Green T, Figurnov M, Ronneberger O, et al. Highly accurate protein structure prediction with AlphaFold. Nature. 2021;596(7873):583–9.
62. Boder ET, Wittrup KD. Yeast surface display for screening combinatorial polypeptide libraries. Nature Biotechnology. 1997;15(6):553–7.

63. Sjostrom DJ, Mohlin C, Ambrosetti E, Garforth SJ, Teixeira AI, Bjelic S. Motif-driven protein binder design towards transferrin receptor helical domain. FEBS J. 2022;289(10):2935–47.